

Thermodynamics of boson systems related to Dunkl differential-difference operators

Marcelo R. Ubriaco*

Laboratory of Theoretical Physics
Department of Physics
University of Puerto Rico
Río Piedras Campus
San Juan
PR 00931, USA

Abstract

We study the thermodynamics of systems based on a Fock space representation inspired by the differential-difference operators proposed in Ref. [1]. We calculate thermodynamic functions as the entropy and heat capacity and compare them with the standard boson case. A calculation of the second virial coefficient and the scalar curvature in two and three dimensions show that these systems becomes repulsive within an interval of negative values of the reflection operator parameter μ_0 . In addition, the stability of this system is examined as a function of μ_0 .

1 Introduction

Our work uses as a starting point the differential-difference operator defined in Ref. [1] and used to study the kernel solutions of the corresponding Laplacian which are known as h -harmonic functions. This work was then extended in Refs.[2]. The differential-difference operator is written

$$\mathcal{D}_x = \frac{\partial}{\partial x} + \frac{\mu_0}{x}(1 - R_x), \quad (1)$$

where μ_0 is a parameter and the operator R_x is a reflection operator which can be formally written as $R_x = (-1)^{x\partial/\partial x}$. More recently, in Refs.[3]-[4] this operator was used to study the solutions and symmetries of a Hamiltonian with an isotropic harmonic potential in two and three dimensions. It was shown

*Electronic address:ubriaco@ltp.uprrp.edu

that this isotropic Dunkl oscillator model is superintegrable and allows separation of variables in the usual coordinate systems with solutions in terms of Hermite, Laguerre and Jacobi polynomials.

This paper is organized as follows. In Section 2 we make a correspondence between the coordinate and the differential-difference operator in Equation 1 with creation and annihilation operators which allow us to define the model we wish to study. In Section 3 we calculate the partition function leading to the entropy, heat capacity functions and critical temperature and compare them with the standard Bose-Einstein (B-E) case. In Section 4 we calculate the second virial coefficients in two and three dimensions, and in Section 5 we calculate the thermodynamic curvature which will tell us about the stability and anyonic behavior of the system. In Section 6 we discuss our results.

2 The model

Our starting point is very simple, we want to study the consequences of proposing a hamiltonian in terms of creation and annihilation operators defined from the correspondence between them and the coordinate and its derivative respectively. Simply, as it is done in the standard case, following the correspondence $a^\dagger \leftrightarrow x$ and $a \leftrightarrow \partial/\partial x$ motivated by their commutation relations we define the hamiltonian

$$\mathcal{H} = \sum_i \epsilon_i \bar{\phi}_i \phi_i, \quad (2)$$

where here the correspondence is given by $\bar{\phi} \leftrightarrow x$ and $\phi \leftrightarrow \mathcal{D}_x$. The commutation relation between ϕ_j and $\bar{\phi}_j$ is simply given by

$$[\phi_i, \bar{\phi}_j] = \delta_{i,j}(1 + 2\mu_0 R_i), \quad (3)$$

Their action on Fock space is

$$\bar{\phi}|n\rangle = \sqrt{n+1}|n+1\rangle, \quad (4)$$

$$\phi|n\rangle = (\sqrt{n} + \frac{\mu_0}{\sqrt{n}})(1 - (-1)^n)|n-1\rangle, \quad (5)$$

and therefore the number operator \mathcal{N}

$$\mathcal{N}|n\rangle = n|n\rangle, \quad (6)$$

if n is even, and

$$\mathcal{N}|n\rangle = (n + 2\mu_0)|n\rangle, \quad (7)$$

for n odd.

By defining the operators:

$$L_1 = (1/2)\bar{\phi}\bar{\phi}, \quad L_{-1} = (1/2)\phi\phi, \quad L_0 = (1/4)(\bar{\phi}\phi + \phi\bar{\phi})$$

we get a representation of the $su(1, 1)$ algebra

$$[L_m, L_n] = (n - m)L_{m+n}. \quad (8)$$

The hamiltonian in Equation 2 in terms of the usual operators a^\dagger and a becomes

$$\mathcal{H} = \sum_i \epsilon_i \left(a_i^\dagger a_i + \mu_0 (1 - (-1)^{\hat{N}_i}) \right), \quad (9)$$

which is clearly hermitian and \hat{N}_i is the usual number operator.

3 Thermodynamic functions

From Equation 9 the partition function for this system is given by

$$\mathcal{Z} = \prod_{l=0} \sum_{n_l=0} e^{-\beta n_l \epsilon_l} e^{-\beta \mu_0 \epsilon_l (1 - (-1)^{n_l})} z^{n_l}, \quad (10)$$

which is easy to sum leading to

$$\mathcal{Z} = \prod_{l=0} \frac{1}{1 - e^{-2\beta \epsilon_l} z^2} (1 + e^{-\beta \epsilon_l} e^{-2\mu_0 \beta \epsilon_l} z). \quad (11)$$

As expected, at $\mu_0 = 0$ we obtain the B-E partition function $Z = \prod_{l=0} \frac{1}{1 - e^{-\beta \epsilon_l} z}$. The average number of particles

$$\langle N \rangle = \frac{1}{\beta} \frac{\partial}{\partial \mu} \ln \mathcal{Z}, \quad (12)$$

$$= \sum_{l=0} \left(\frac{2}{e^{2\beta \epsilon_l} z^2 - 1} + \frac{1}{e^{\beta \epsilon_l} e^{2\mu_0 \beta \epsilon_l} z + 1} \right), \quad (13)$$

In particular, the zero momentum distribution is $\langle n_0 \rangle = \frac{z}{1-z}$, which is identical to the B-E case. Replacing, in the thermodynamic limit, the summation by an integral and expanding in powers of z we obtain

$$\ln \mathcal{Z} = -\ln(1-z) + \frac{1}{\lambda^3} g_{5/2}(\mu_0, z), \quad (14)$$

$$\langle N \rangle = \frac{z}{1-z} + \frac{1}{\lambda^3} g_{3/2}(\mu_0, z), \quad (15)$$

where the functions

$$g_{5/2}(\mu_0, z) = \sum_{n=1} \frac{z^{2n}}{2^{3/2} n^{5/2}} + \left(\frac{1}{1+2\mu_0} \right)^{3/2} \sum_{n=1} \frac{(-1)^{n+1} z^n}{n^{5/2}}, \quad (16)$$

$g_{3/2}(\mu_0, z) = z \frac{\partial}{\partial z} g_{5/2}(\mu_0, z)$ become the standard functions $g_{5/2}(z)$ and $g_{3/2}(z)$ for μ_0 respectively and λ is the thermal wavelength.

Figure 1 is a graph of the functions $g_{5/2}(\mu_0, 1)$ and $g_{3/2}(\mu_0, 1)$ in the interval $0 \leq \mu_0 \leq 1$ showing that their values within this interval are smaller than the textbook, $\mu_0 = 0$, functions. These functions become singular at $\mu_0 = -0.5$ and

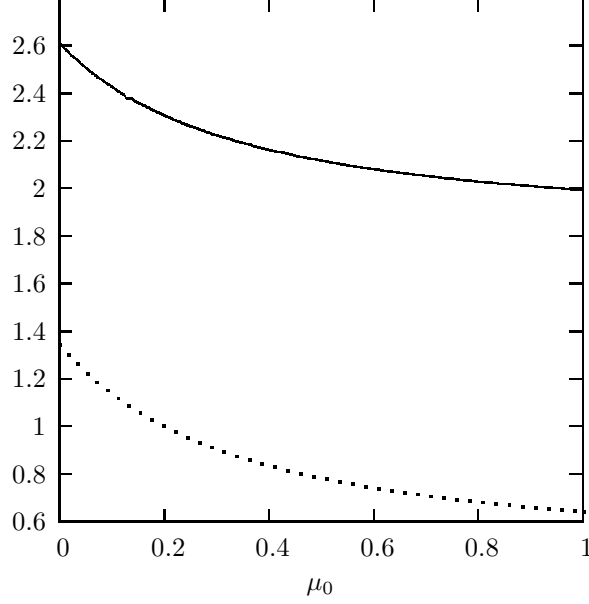


Figure 1: The functions $g_{3/2}(\mu_0, 1)$ (solid line) and $g_{5/2}(\mu_0, 1)$ (dotted line) for $z = 1$ and the parameter $0 \leq \mu_0 \leq 1$

complex for $\mu_0 < -0.5$ restricting therefore the range of values to the interval $\mu_0 > -0.5$.

The critical temperature

$$T_c = \frac{h^2}{2\pi m k} \left(\frac{\langle N \rangle}{V g_{3/2}(\mu_0, 1)} \right)^{2/3}. \quad (17)$$

Since for $\mu_0 > 0$ the function $g_{3/2}(\mu_0, 1) < g_{3/2}(1)$ the critical temperature T_c is higher than the critical temperature for B-E case T_c^{BE} . For $-0.5 < \mu_0 < 0$, $g_{3/2}(\mu_0, 1) > g_{3/2}(1)$ and therefore $T_c < T_c^{BE}$ which means that the system is less attractive. In general

$$\frac{T_c}{T_c^{BE}} = \left(\frac{2.612}{g_{3/2}(\mu_0, 1)} \right)^{2/3}, \quad (18)$$

and in the range $0 \leq \mu_0 \leq 1$ the quotient $\frac{T_c}{T_c^{BE}}$ takes values in the interval $1 \leq \frac{T_c}{T_c^{BE}} \leq 1.2$. For values $\mu_0 \gg 0$ the function $g_{3/2}(\mu_0, 1) \approx \frac{1}{\sqrt{2}} g_{3/2}(1)$ and the ratio $\frac{T_c}{T_c^{BE}} \approx 1.26$. Denoting as S_+ and S_- the entropies above and below the critical temperature respectively, we write

$$\lim_{V \rightarrow \infty} \frac{S_+}{V} = \frac{5}{2} \frac{k}{\lambda^3} g_{5/2}(\mu_0, z) - \frac{k \langle N \rangle}{V} \ln z, \quad (19)$$

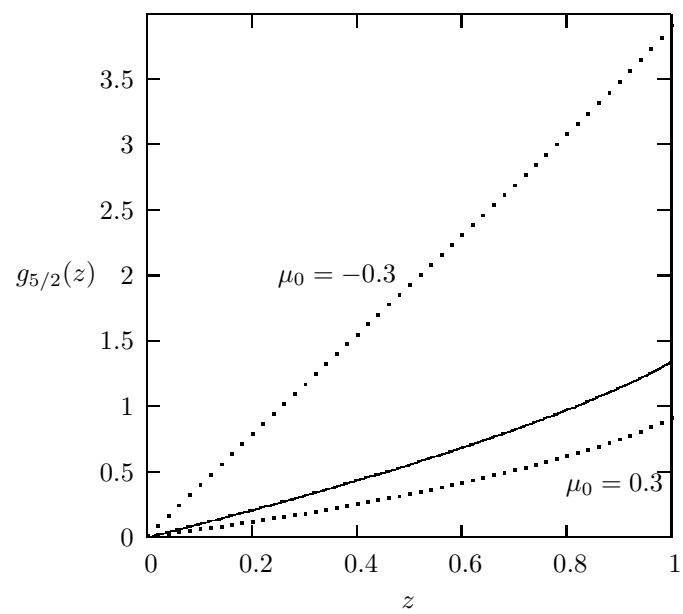


Figure 2: The function $g_{5/2}(\mu_0, z)$ for $\mu_0 = -0.3, \mu_0 = 0$ (solid line) and $\mu_0 = 0.3$ in the interval $0 \leq z \leq 1$

$$\lim_{V \rightarrow \infty} \frac{S_-}{V} = \frac{5}{2} \frac{k}{\lambda^3} g_{5/2}(\mu_0, 1), \quad (20)$$

Figure 2 shows a graph of the function $g_{5/2}(\mu_0, z)$ for three values of the parameter μ_0 . For $\mu_0 < 0$ the function $g_{5/2}(\mu_0, z) > g_{5/2}(z)$ and the entropies S_+ and S_- are larger than S^{BE} . In the interval $\mu_0 > 0$ the entropies $S_{\pm} < S^{BE}$. Similarly to the standard case the heat capacity above and below the critical temperature is written

$$C_+ = \frac{15}{4} \frac{k}{\lambda^3} g_{5/2}(\mu_0, z) - \frac{9}{4} \frac{k \langle N \rangle}{V} \frac{g_{3/2}(\mu_0, z)}{g_{1/2}(\mu_0, z)}, \quad (21)$$

$$C_- = \frac{15}{4} \frac{k}{\lambda^3} g_{5/2}(\mu_0, 1). \quad (22)$$

Since the quotient $\frac{g_{3/2}(\mu_0, z)}{g_{1/2}(\mu_0, z)}$ is, independently of the value of μ_0 , almost constant for low z we have that for $\mu_0 < 0$ ($\mu_0 > 0$) the heat capacity $C_{\pm} > C^{BE}$ ($C_{\pm} < C^{BE}$).

4 Virial coefficients

In this Section we calculate the second virial coefficients in two and three dimensions. For $D = 3$, we expand

$$\ln \mathcal{Z} = \frac{4\pi V}{h^3} \int_0^\infty dp p^2 \left(-\ln(1 - e^{-\beta p^2/m} z^2) + \ln(1 + e^{-\beta p^2/2m} e^{-\mu_0 \beta p^2/m} z) \right), \quad (23)$$

Expanding the integrand in powers of z and solving the elementary integrals gives

$$\ln \mathcal{Z} = \frac{V}{\lambda^3} \left(\frac{z}{(1 + 2\mu_0)^{3/2}} + \frac{\delta(\mu_0)}{(1 + 2\mu_0)^3} z^2 + \dots \right), \quad (24)$$

where $\delta(\mu_0) = \frac{1}{2^{3/2}} ((1 + 2\mu_0)^3 - (1/2)(1 + 2\mu_0)^{3/2})$. Performing a similar expansion for $\langle N \rangle$ and after writing the fugacity z in powers of $\langle N \rangle$ lead to the result

$$pV = kT \langle N \rangle \left(1 - \delta(\mu_0) \left(\frac{h^2}{2m\pi kT} \right)^{3/2} \frac{\langle N \rangle}{V} + \dots \right). \quad (25)$$

A similar calculation for $D = 2$ gives

$$pA = kT \langle N \rangle \left(1 - \eta(\mu_0) \left(\frac{h^2}{2m\pi kT} \right) \frac{\langle N \rangle}{A} + \dots \right), \quad (26)$$

Figure 3 shows a graph of the second virial coefficients for $D = 3$ (solid line) and $D = 2$ (dotted line) for $-0.5 \leq \mu_0 \leq 0.1$. The coefficient $\delta(0) = 1/2^{5/2}$, which is the second virial coefficient for the B-E case. The system behaves as an ideal gas, $\delta(\mu_0) = 0$, at the values $\mu_0 = -0.5$ and $\mu_0 = -0.185$, and between these

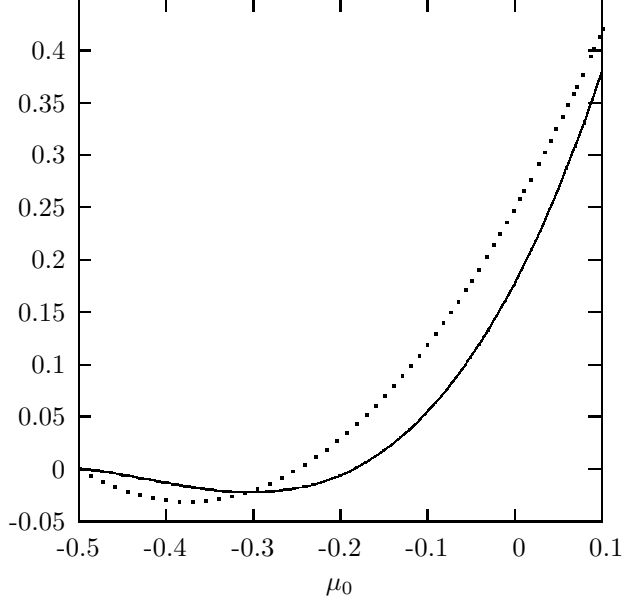


Figure 3: The virial coefficients $\delta(\mu_0)$ for $D = 3$ (solid line), and $\eta(\mu_0)$ for $D = 2$ (dotted line) as a function of the parameter $-0.5 \leq \mu_0 \leq 0.5$

two values the coefficient $\delta(\mu_0)$ is negative and the system becomes repulsive reaching the lowest value $\delta(-0.3) = -0.022$. Therefore the interpolation from bosonic to fermionic behavior does not reach the free fermion limit $\delta = -1/2^{5/2}$. The switch from bosonic to fermionic behavior when the parameter $\mu_0 < 0$ is consistent with the fact that the critical temperature is larger than T_c^{BE} for $-0.5 < \mu_0 < 0$.

For $D = 2$, the ideal gas case is reached at the values $\mu_0 = -0.5$ and $\mu_0 = -0.25$ and between these two values the virial coefficient $\eta(\mu_0)$ becomes negative but without reaching the free fermion value $\eta = -1/4$. For those values $\mu_0 \gg 0$ the virial coefficients functions increase as: $\delta(\mu_0) = 2^{3/2}\mu_0^3$ and $\eta(\mu_0) = 2\mu_0^2$. Although this system exhibits anyonic behavior in two and three dimensions, the parameter μ_0 does not interpolate completely between the free boson and fermion limits.

5 Thermodynamic curvature

In this section we calculate the thermodynamic curvature R , which is basically the two dimensional curvature in the parameter space spanned by the variables $\beta_1 = \beta$ and $\beta_2 = -\beta\mu$. The basic geometrical approach to thermodynamics

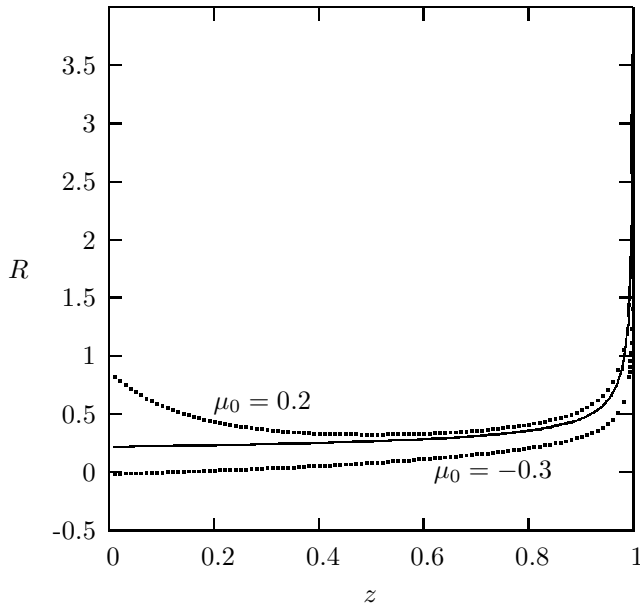


Figure 4: The scalar curvature R at $D = 3$, in units of $\lambda^3 V^{-1}$, as a function of the fugacity z at constant β for the parameter values $\mu_0 = -0.3, 0.2$ and the standard case $\mu_0 = 0$ (solid line).

was initiated in Refs.[5]-[9] and extended in [10]-[19] to define a metric and the scalar curvature as a measure of the correlations strength of the system. There have been numerous applications of this formalism including classical and quantum gases [20]-[23], magnetic systems [24]-[27], non-extensive statistical mechanics [28]-[30], anyon gas, fractional statistics and deformed boson and fermion systems [31], systems with fractal distribution functions [32], quantum group invariant systems [33] and systems with M -statistics [34]. A calculation of the scalar curvature tell us not only whether the system is attractive (repulsive) from its values $R > 0$ ($R < 0$) but also about its stability which is obtained from its departure from the classical gas value $R = 0$. For exponential probability distributions, the metric is simply defined as

$$g_{\alpha\gamma} = \frac{\partial^2 \ln Z}{\partial \beta^\alpha \partial \beta^\gamma}, \quad (27)$$

and the two dimensional scalar curvature follows from the basic relation

$$R = \frac{2}{\det g} R_{1212}, \quad (28)$$

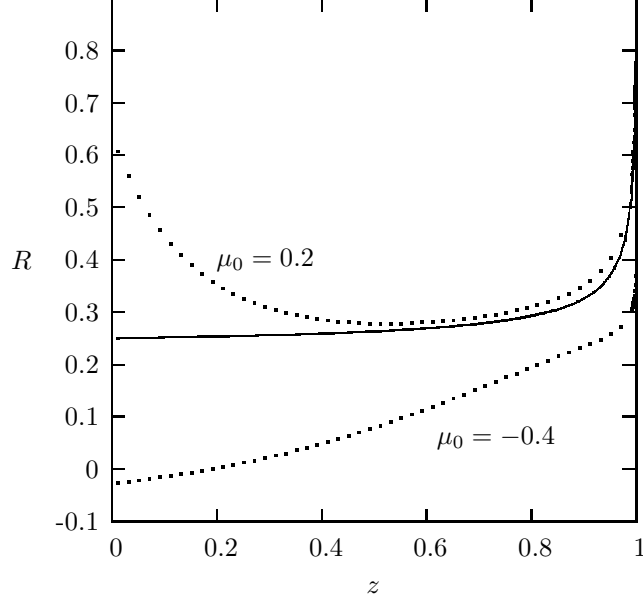


Figure 5: The scalar curvature R at $D = 2$, in units of $\lambda^2 A^{-1}$, as a function of the fugacity z at constant β for the parameter values $\mu_0 = -0.4, 0.2$ and the standard case $\mu_0 = 0$ (solid line).

where $\det g = g_{11}g_{22} - g_{12}g_{12}$. Due to the obvious identities $\frac{\partial g_{ij}}{\partial \beta^j} \equiv g_{ij,j} = g_{jj,i}$ the curvature tensor R_{ijkl} reduces to

$$R_{ijkl} = g^{mn} (\Gamma_{mil} \Gamma_{njk} - \Gamma_{mik} \Gamma_{njl}), \quad (29)$$

where the Christoffel symbol $\Gamma_{ijk} = \frac{1}{2}g_{ij,k}$. The curvature R is simply given by the determinant

$$R = \frac{1}{2(\det g)^2} \begin{vmatrix} g_{11} & g_{22} & g_{12} \\ g_{11,1} & g_{22,1} & g_{21,1} \\ g_{11,2} & g_{22,2} & g_{21,2} \end{vmatrix}. \quad (30)$$

The metric components are readily calculated from Equation 23

$$g_{11} = C\left(\frac{D}{2}\right)\left(\frac{D}{2} + 1\right)\frac{1}{\beta^{\frac{D}{2}+2}}I_1, \quad (31)$$

$$g_{12} = -C\left(\frac{D}{2}\right)\frac{1}{\beta^{\frac{D}{2}+1}}I_2, \quad (32)$$

$$g_{22} = \frac{C}{\beta^{D/2}}I_3, \quad (33)$$

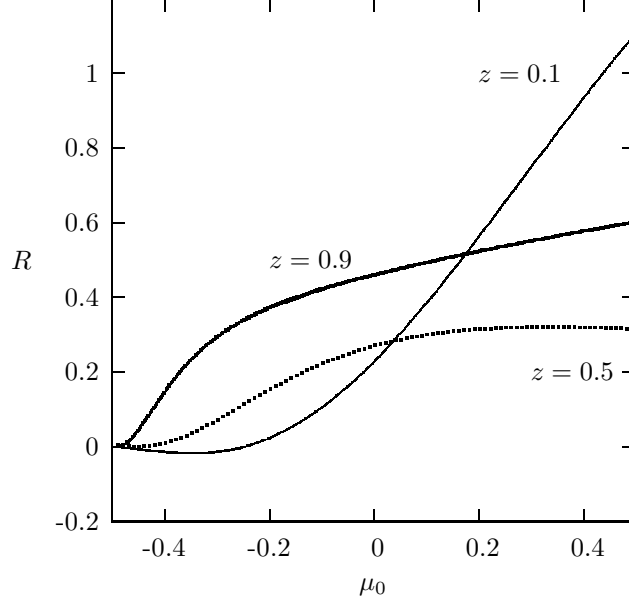


Figure 6: The scalar curvature R at $D = 3$, in units of $\lambda^3 V^{-1}$, as a function of the parameter μ_0 for values of the fugacity $z = 0.1, 0.5, 0.9$.

where the constant $C = \frac{4\pi m A}{h^2}$ for $D = 2$, and $C = 4\pi V \left(\frac{2m}{h^2}\right)^{3/2}$ for $D = 3$. The integrals are given by

$$I_1 = \int_0^\infty dx x^{D-1} (-\ln f + \ln g), \quad (34)$$

$$I_2 = \int_0^\infty dx x^{D-1} \left(\frac{2(f-1)}{f} - \frac{g-1}{g} \right), \quad (35)$$

$$I_3 = \int_0^\infty dx x^{D-1} \left(\frac{4(1-f)}{f} + \frac{4(1-f)^2}{f^2} + \frac{g-1}{g} - \frac{(g-1)^2}{g^2} \right) \quad (36)$$

with the functions $f = 1 - e^{-2x^2} z^2$ and $g = 1 + e^{-(1+2\mu_0)x^2} z$. From Equation 30 we obtain

$$R = \frac{\lambda^D}{V_D} \frac{\pi^{D/2-1}}{2^{D-1}} (D+2) \frac{I_3 I_2^2 - 2I_1 I_3^2 + I_1 I_2 I_4}{((D+2)I_1 I_3 - D I_2^2)^2}, \quad (37)$$

where V_D stands for the area or volume.

Figure 4 shows a graph of the scalar curvature R for the three dimensional case as a function of the fugacity z . For values such that $\mu_0 < 0$ the system becomes repulsive at high temperatures ($z \approx 0$) and it is more stable than the B-E case for all values of z . For $\mu_0 > 0$ the system is always bosonic and it becomes

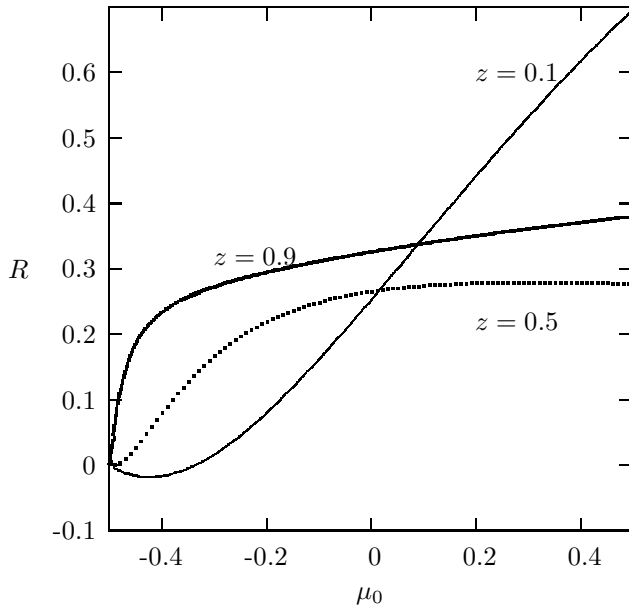


Figure 7: The scalar curvature R at $D = 2$, in units of $\lambda^2 A^{-1}$, as a function of the parameter μ_0 for values of the fugacity $z = 0.1, 0.5, 0.9$.

mora unstable at high temperatures. As expected, there is a singularity in R as $z \rightarrow 1$ at the onset of Bose-Einstein condensation. For the two dimensional case the behavior of R as a function of z , as shown in Figure 5, is quite similar to the three dimensional case. Figures 6 and 7 are graphs of the scalar curvature R as a function the parameter μ_0 for the values of $z = 0.1, 0.5, 0.9$ for the three and two dimensional cases respectively. Independently of the value of the fugacity the curvature vanishes at $\mu_0 = -0.5$ which is the value that corresponds to the classical, Maxwell-Boltzmann case. At high temperatures, there is another value of μ_0 such that the behavior becomes classical, as for example for $z = 0.1$ the curvature $R = 0$ at $\mu_0 \approx -0.25$, and within the interval $-0.5 < \mu_0 < 0.25$ the curvature becomes negative. At low temperatures the system is attractive independently of μ_0 . Independently of the value of z , the instability increases as μ_0 increases. In general, systems with $\mu_0 > 0$ are more unstable and therefore more correlated than those with $\mu_0 < 0$.

6 Conclusions

In this manuscript we have proposed a thermodynamic model based on a Fock space defined by making a correspondence with the so called Dunkl differential-

difference operators. The partition function and the occupation number are written in terms of two functions $g_{5/2}(\mu_0, z)$ and $g_{3/2}(\mu_0, z)$ respectively which become the standard $g_{5/2}(z)$ and $g_{3/2}(z)$ as the parameter $\mu_0 \rightarrow 0$. These two new functions $g_\eta(\mu_0, z)$ impose a lower limit $\mu_0 > -0.5$ as a result that they become complex for $\mu_0 < -0.5$. A numerical calculation of these functions shows that the critical temperature is higher (lower) than the B-E case $\mu_0 = 0$ for the range of values $\mu_0 > 0$ ($-0.5 < \mu_0 < 0$). The fact that the expressions for the entropy and heat capacity are identical than the standard case but written in terms of these new functions $g_\eta(\mu_0, z)$ help us to conclude that these thermodynamic functions are larger (lower) than the B-E for $\mu_0 < 0$ ($\mu_0 > 0$). A calculation of the virial coefficients for $D = 2$ and $D = 3$ show that they vanish at two values of the parameter μ_0 mimicking therefore the behavior of a classical system. Between these two values the virial coefficient becomes negative and therefore the system becomes repulsive but without reaching the Fermi-Dirac value of $-\frac{1}{2^{5/2}}$ and $-1/4$ for $D = 3$ and $D = 2$ respectively. These results are consistent with the fact that, for example, the entropy function is larger for $\mu_0 < 0$ than for $\mu_0 \geq 0$. A calculation of the thermodynamic curvature R gave us a larger picture about the attractive or repulsive behavior and the stability as a function of either the parameter μ_0 or the fugacity z . For all temperature values the curvature graph shows a more (less) correlated system for positive (negative) values of μ_0 as compared with the B-E case. In addition, at low temperatures the behavior is bosonic independently of the value of μ_0 and it becomes more unstable than the B-E case for all values of $\mu_0 > 0$. Therefore, by making a correspondence between Dunkl differential-difference operators with creation and annihilation operators we have proposed a thermodynamic model that exhibits anyonic behavior in two and three dimensions. Although this model does not interpolates completely between the B-E and F-D cases it certainly gives a new approach wherein anyonic behavior manifest in three dimensions other than previously proposed models based on M -statistics [35] and quantum group invariance [36]

References

- [1] C. F. Dunkl, Trans. Amer. Math. Soc. 311 (1989) 167.
- [2] C. F. Dunkl, J. Phys. A:Math. Gen. 35 (2002) 10391.
C. F. Dunkl, arXiv:1210.3010.
- [3] V. X. Genest, M. E.H. Ismail, L. Vinet and A. Zhedanov, J. Phys. A: Math. Theor. 46 (2013) 145201; arXiv:1302.6142.
- [4] V. X. Genest, L. Vinet and Alexei Zhedanov, arXiv:1312.3877.
- [5] L. Tisza, Generalized Thermodynamics (MIT, Cambridge, 1966).
- [6] R. B. Griffiths and J. C. Wheeler, Phys. Rev. A 2(1970) 1047.

- [7] F. Weinhold, J. Chem. Phys. 63 (1975) 2479.
- [8] S.-I. Amari, Differential-Geometrical Methods in Statistics (Springer-Verlag, Berlin, 1985).
- [9] S.-I. Amari and H. Nagaoka, Methods of Information Geometry (AMS, Rhode Island, 2000).
- [10] R. S. Ingarden, H. Janyszek, A. Kossakowski and T. Kawaguchi, Tensor N.S. 37 (1982) 105.
- [11] W. K. Wootters, Phys. Rev. D 23 (1981) 357.
- [12] R. Gilmore, Phys. Rev. A 30 (1984) 1994.
- [13] G. Ruppeiner, Phys. Rev. A 32 (1985) 3141.
- [14] R. Gilmore, Phys. Rev. A 32 (1985) 3144.
- [15] J. Nulton, P. Salamon, Phys. Rev. A 31 (1985) 2520.
- [16] H. Janyszek, Rep. Math. Phys. 24 (1986) 1; Rep. Math. Phys. 24 (1986) 11.
- [17] H. Janiszek and R. Mrugala, Rep. Math. Phys. 27 (1989) 145.
- [18] G. Ruppeiner, Rev. Mod. Phys. 67 (1995) 605.
- [19] G. Ruppeiner, Am. J. Phys. 78 (2010) 1170, and references therein.
- [20] G. Ruppeiner, Phys. Rev. A 20 (1979) 1608.
- [21] J. Nulton, P. Salamon, Phys. Rev. A 31 (1985) 2520.
- [22] H. Janiszek and R. Mrugala, J. Phys. A: Math. Theor. 23 (1990) 467.
- [23] D. Brody and D. Hook, J. Phys. A: Math. Theor. 42 (2009) 023001.
- [24] H. Janiszek and R. Mrugala, Phys. Rev. A 39 (1989) 6515.
- [25] H. Janyszek, J. Phys. A: Math. 23 (1990) 477.
- [26] D. Brody and N. Rivier, Phys. Rev. E 51 (1995) 1006.
- [27] W. Janke, D. A. Johnston and R. Kenna, Physica A 336 (2004) 181.
- [28] R. Trasarti-Battistoni, cond-mat/0203536.
- [29] M. Portesi, A. Plastino and F. Pennini, Physica A 365 (2006) 173.
- [30] A. Ohara, Phys. Lett. A 370 (2007) 184.
- [31] B. Mirza and H. Mohammadzadeh, Phys. Rev. E 79 (2008) 021127; Phys. Rev. E 80 (2009) 011132; Phys. Rev. E 82 (2010) 031137; J. Phys. A: Math. Theor. 44 (2011) 475003.

- [32] M. R. Ubriaco, Phys. Lett. A 376 (2012) 2899.
- [33] M. R. Ubriaco, Phys. Lett. A 376 (2012) 3581.
- [34] M. R. Ubriaco, Physica A 392 (2013) 4868.
- [35] W. Chen, Y. Jack Ng and H. Van Dam, Mod. Phys. Lett. A 11 (1996) 795.
- [36] M. R. Ubriaco, Phys. Rev. E 55 (1997) 291.